Observation of pristine Majorana bound state
in iron-based superconductor

Dongfei Wang[1,2†], Lingyuan Kong[1,2†], Peng Fan[1,2†], Hui Chen[1], Yujie Sun[1], Shixuan Du[1,3], John Schneeloch[4], Ruidan Zhong[4], Genda Gu[4], Liang Fu[5], Hong Ding[1,2,3*], and Hongjun Gao[1,2,3*]

[1]Beijing National Laboratory for Condensed Matter Physics and Institute of Physics, Chinese Academy of Sciences, Beijing 100190, China

[2]School of Physical Sciences, University of Chinese Academy of Sciences, Beijing 100190, China

[3]Collaborative Innovation Center of Quantum Matter, Beijing 100190, China

[4]Condensed Matter Physics and Materials Science Department, Brookhaven National Laboratory, Upton, New York 11973, USA

[5]Department of Physics, Massachusetts Institute of Technology, Cambridge, Massachusetts 02139, USA

†These authors contributed equally to this work

*Correspondence to: dingh@iphy.ac.cn, hjgao@iphy.ac.cn

The search for Majorana bound state (MBS) has recently emerged as one of most active research areas in condensed matter physics, due to its non-Abelian statistics which can be used for robust quantum computation. A highly sought-after platform for MBS is two-dimensional topological superconductors, where MBS is predicted to exist as a zero-energy mode in the core of a vortex. A clear observation of MBS, however, is often hindered by the presence of additional low-energy bound states inside the vortex core. By using scanning tunneling microscope on the newly discovered superconducting topological surface state of iron-based superconductor $FeTe_{1-x}Se_x$ (x = 0.45, T_c = 14.5 K), we unequivocally observe a pristine MBS inside a vortex core, well separated from non-topological bound states which are pushed away from zero energy due to the high ratio between the superconducting gap and the Fermi energy in this material. This observation offers a new, robust platform for realizing and manipulating Majorana bound states at a relatively high temperature.

Majorana bound state (MBS) in condensed matter systems has attracted tremendous interest due to its non-Abelian statistics and potential applications in topological quantum computation *(1,2)*. MBS is theoretically predicted to emerge as a spatially localized zero-energy mode in certain *p*-wave topological superconductors in one and two dimensions *(3,4)*. While the material realization of such *p*-wave superconductors has remained elusive, new platforms for MBS have recently been proposed at the interface of conventional *s*-wave superconductors and topological insulators *(5)*, nanowires *(6 - 8)*, or atomic chains *(9)*, where the proximity effect on a spin-non-degenerate band induces a topological superconducting state. While various

experimental signatures of MBS have been observed in such systems *(10 - 13)*, a clear detection and manipulation of MBS are hindered by the small ratio of the topological superconducting (SC) gap (Δ_{sc}) over the Fermi energy (E_F) and the complicated material interface problems.

Very recently, using high-resolution angle-resolved photoemission spectroscopy (ARPES), we have discovered a new platform for MBS in a bulk superconductor $FeTe_{0.55}Se_{0.45}$ (T_c = 14.5 K), which naturally has spin-helical Dirac fermion surface states with a full superconducting gap (Δ_{sc} = 1.8 meV) *(14)*, fulfilling all the required conditions for MBS *(5)*. The combination of high-T_c superconductivity and superconducting topological surface states in a single material removes the challenging interface problems in previous proposals, offering clear advantages for detecting and manipulating MBS. More importantly, the superconducting surface state has an extremely large Δ_{sc}/E_F ratio. Under this condition, the zero-energy MBS in a vortex core is expected to be well separated in energy from Caroli-de Gennes-Matricon states *(15)*.

Motivated by the above considerations, we carry out a high-resolution scanning tunneling microscopy/spectroscopy (STM/S) experiment on the surface of $FeTe_{0.55}Se_{0.45}$ (T_c = 14.5 K) under a magnetic field of 4 T along the c-axis and a low temperature of 0.55 K. The single crystals in this study are from the same and similar batches of single crystals as in our previous ARPES study *(14)*, making comparison between them more reliable and meaningful. We start with Fig.1 by demonstrating a zero-energy peak emerging at the center of a vortex core on the superconducting surface of $FeTe_{0.55}Se_{0.45}$, whose crystal structure is shown in Fig. 1A. In Fig. 1B, we display a topographic STM image with atomic resolution on an area of surface that has no visible impurities or defects under a 4T magnetic field. A zero-biased tunneling current derivative or conductance (dI/dV) map, as shown in Fig. 1C, clearly display an array of vortex cores roughly situated at a triangular Abrikosov lattice. We contrast the density of state (DOS) inside and outside of core in Fig. 1D. Outside of the core, we clearly observe a superconducting spectrum with multiple gap features, at ±1.8, ±2.5 meV, respectively, similar to the ones observed by previous STM studies on similar single crystals *(16,17)*. These different SC gaps correspond well with different SC gaps on different Fermi surfaces of this material observed by previous ARPES studies. The 1.8-meV gap (Δ_1) corresponds to the gap observed at the Brillouin zone center (Γ), which is the induced superconducting gap of the topological surface state *(14)*, and the 2.5-meV gap (Δ_2) corresponds to the gap observed on a larger hole-like Fermi surface around Γ *(18)*. Note the 4-meV gap (Δ_3) on the electron-like Fermi surface at the zone corner (M) is seldom observed by STM possibly due to the fact that the tunneling matrix is more sensitive to the states with small k vectors. At the edge of the core, the magnitudes of SC gaps appear largely unchanged, although the spectrum shapes seem to be different. At the center of the core, we observe a strong zero-biased peak (ZBP) with the full width at half maximum (FWHM) of 0.5 meV and the amplitude of 2.4 relative to the background just outside the gapped region. We note a similar ZBP was reported previously *(17)*.

We then demonstrate in Fig. 2 that the ZBP observed does not split when moving

away from the core center. On the regions where patches of vortex cores are clearly visible we often observe ZBPs inside the vortex cores. In Fig. 2 we display results from three vortex cores on different surface regions of a single crystal of $FeTe_{0.55}Se_{0.45}$, where strong ZBPs are observed. In Figs. 2A–C, we plot zero-biased conductance maps for the three vortex cores. The three vortex cores have similar shape and size, appearing as an irregular oval shape with a visible size of about 10 nm in diameter and a bright spot in the vicinity of the core center. We carry out dI/dV measurements along a line going through the brightest spot inside the core for each of three cores, and display the corresponding intensity plots in Figs. 2D-F. It is visually evident that these ZBPs remain at the zero energy until their intensity fades away outside the vortex core. The lines of ZBP extend for a length of about 8 nm for all three cores, situating at the zero energy with the experimental energy uncertain of approximately 0.1 meV. In the meantime, the smaller SC gap, as indicated by the bright stripes around ±2 meV, shrinks in size and reduces in intensity along the same 8-nm length inside the core.

The non-split ZBP inside a vortex core agrees with the expected behavior of an isolated and pure Majorana bound state in a vortex core of a topological superconductor. To reveal the spatial profile of the MBS, in Fig. 3 we closely examine its intensity as a function of energy and position and compare it to theoretical calculations. We display all the 93 dI/dV spectra measured along the linecut shown in Fig. 2C in a waterfall-like plot in Fig. 3A, select 9 spectra evenly from the core center to the edge for an overlapping plot in Fig. 3B, and construct a 3-dimensional drawing of dI/dV(E, r) in Fig. 3C. These plots clearly show a single dI/dV peak at the zero energy inside a vortex core. The peak intensity has a distinctive spatial profile as displayed in Fig. 3D, which maps out the wave function of MBS. From a single exponential decay fit shown in Fig. 3D, we obtain the decay length (λ) of the ZBP around 3 nm. We also fit the linewidth of MBS and find a surprising result that the FWHM of MBS decreases from ~ 0.4 meV at the core center to ~ 0.2 meV near the core edge, also as shown in Fig. 3D. Such the unusual linewidth of MBS inside a vortex core may be the result of interplay between tunnel-induced broadening and temperature as predicted theoretically *(19)*. Furthermore, the peak intensity is found to anti-correlate with the SC gap size: upon approaching the vortex core, the SC gap rapidly decreases from 1.8 meV to 1.3 meV and the coherence peak at the gap edge shrinks significantly, as can be seen in Figs. 3A-C. We also notice that from the intensity plots of Figs. 2 A-C, the MBS intensity map is slightly elongated along one of the Te-Te directions, indicating a possible nematicity for the MBS in this material.

Our clear observation of a pristine MBS in a vortex core of this superconductor is likely enabled by the large Δ_{sc}/E_F ratio. In a usual topological insulator/superconductor heterostructure, this ratio is tiny, on the order of $10^{-3} - 10^{-2}$. This has been shown to induce, in addition to the MBS at the zero energy, many Caroli–de Gennes–Matricon bound states (CBSs), whose level spacing is proportion to Δ_{sc}^2/E_F. As a result, these CBSs crowdedly pack very close to the zero energy, obscuring a clean detection of MBS from the dI/dV spectra. In our previous high-resolution ARPES study on $FeTe_{0.55}Se_{0.45}$, we have convincingly demonstrated that

this iron-based superconductor posses a superconducting topological surface state by showing 1) a non-trivial band inversion at Γ, 2) a Dirac-cone dispersion of the surface state at Γ, 3) a helical spin structure of the surface state, 4) an isotropic SC gap on the surface state with a magnitude of 1.8 meV, as schematically summarized in Fig. 4A. From the ARPES plot of surface and bulk dispersion around Γ, adopted from Ref. (14) and replotted in the left panel of Fig. 4B, the ratio of Δ_{sc}/E_F is about 0.4, significantly larger than the one in any other topological superconducting systems. We also obtain independent evidence for the superconducting Dirac surface states from our STM measurement, as shown in the right panel of Fig. 4B. We notice that the bump at -14.9 meV in the STM spectrum corresponds to the top of bulk valence band in the ARPES plot, and the dip at $-$ 4.4 meV in STM matches to the Dirac crossing in ARPES. Remarkably, we observe a peak at $+$ 6.1 meV in the STM spectrum, which is the exact energy of the bottom of bulk conduction band by symmetry. This large Δ_{sc}/E_F ratio is expected to push most if not all CBSs far away from the zero energy, leaving the MBS isolated and unspoiled, as illustrated schematically in Fig. 4C. We also note that all the bulk bands in this multi-band material have fairly small values of E_F, ranging from a few to a few tens meV, thus their Δ_{sc}/E_F ratios are also fairly sizable given the large bulk superconducting gaps (Δ_2 = 2.5 meV, Δ_3 = 4 meV) in this material, which are among the highest among all the known topological superconductors.

Finally we make a comparison between theoretical calculated MBS spatial decay profile with the observed one in Fig. 4D. The theoretical profile of MBS can be obtained by solving the de Gennes equation analytically (5,20) or numerically (21,22) as in previous theoretical works. Using either a gap profile model for the one shown in Fig. 3D or a constant gap model in our calculation, we find both models yield almost identical decay profiles. By using the parameters of E_F = 4.4 meV, Δ_{sc} = 1.8 meV, and $\xi_0 = v_F/\Delta_{sc}$ = 10 nm, which are obtained directly from our STM and ARPES results (14), the theoretical MBS profile matches remarkably well with the experimental one. This quantitative agreement between theoretical prediction and experimental observation strongly supports the existence of a pristine Majorana bound state inside the vortex core of this intrinsic topological superconducting system. In particular, we note that the FWHM of the observed MBS spatial distribution λ = 3 nm is much shorter than the coherence length ξ_0 = 10 nm, a nontrivial result agreeing with the theoretically calculated MBS wave function (20).

The observation of a pristine MBS in an iron-based superconductor has important implications for both iron-based superconductors and Majorana fermion research. First, it brings an interesting and unexpected "topological" aspect to iron-based superconductivity. This new aspect may yield important clues for the pairing symmetry or even the mechanism of unconventional superconductivity in Fe(Te, Se). It is also worth noting that Fe(Te, Se) has the largest electron correlation among the iron-based superconductors, which decreases the Fermi energy values of all its bands and brings the system close to the BEC regime. Second, the high transition temperature and the large gap in this superconductor bring a new and widely available venue for Majorana research based on natural-occurring quantum materials. This

discovery of the pristine MBS on the surface of high-T_c iron-based superconductor offers an ideal platform for detailed studies of MBS properties and possibly robust and high-density devices for topological quantum computation.

References:

1. A. Y. Kitaev, Ann. Phys. **303**, 2 (2003)
2. Nayak, S. H. Simon, A. Stern, M. Freedman, and S. Das Sarma, Rev. Mod. Phys. **80**, 1083 (2008)
3. A. Y. Kitaev, Physics-Uspekhi. **44**, 131 (2001)
4. N. Read and D. Green, Phys. Rev. B **61**, 10267 (2000)
5. L. Fu and C. L. Kane, Phys. Rev. Lett. **100**, 096407 (2008)
6. R. M. Lutchyn, J. D. Sau, and S. Das Sarma, Phys. Rev. Lett. **105**, 077001 (2010)
7. Y. Oreg, G. Refael, and F. von Oppen, Phys. Rev. Lett. **105**, 177002 (2010)
8. Andrew C. Potter and Patrick A. Lee, Phys. Rev. Lett. **105**, 227003 (2010)
9. S. Nadj-Perge, I. K. Drozdov, B. A. Bernevig, and Ali Yazdani, Phys. Rev. B **88**, 020407 (2013)
10. V. Mourik et al., Science **336**, 1003 (2012)
11. Stevan Nadj-Perge et al., Science **346**, 602 (2014)
12. Hao-Hua Su et al., Phys. Rev. Lett. **116**, 257003 (2016)
13. M. T. Deng et al., Science **354**, 1557 (2016)
14. P. Zhang et al., https://arxiv.org/abs/1706.05163 (2017)
15. C. Caroli, P. G. de Gennes, and J. Matricon, Phys. Lett. **9**, 307 (1964)
16. T. Hanaguri, S. Niitaka, K. Kuroki, and H. Takagi, Science **328**, 474 (2010)
17. F. Massee et al., Sci. Adv. **1**, e1500033 (2015)
18. H. Miao et al., Phys. Rev. B **85**, 094506 (2012)
19. K. T. Law, Patrick A. Lee, and T. K. Ng, Phys. Rev. Lett. **103**, 237001 (2009)
20. Yuxuan Wang and L. Fu, https://arxiv.org/abs/1703.06880 (2017)
21. Ching-Kai Chiu, Matthew J. Gilbert, and Taylor L. Hughes, Rev. B **84**, 144507 (2011)
22. Lun-Hui Hu, Chuang Li, Dong-Hui Xu, Yi Zhou, and Fu-Chun Zhang, Phys. Rev. B **94**, 224501 (2016)
23. G. Xu et al., Phys. Rev. Lett. **117**, 047001 (2016)
24. Jinsheng Wen et al, Phys. Rev. B **80**, 104506 (2009)

Materials and Methods:

Large single crystals of $FeTe_{0.55}Se_{0.45}$ with high quality were grown using the self-flux method, and their values of T_c were determined to be 14.5 K from magnetization measurements *(24)*. The samples used in the experiments were cleaved *in situ* and immediately transferred to the STM head. Experiments were performed in an ultrahigh vacuum (1×10^{-11} mbar) LT-STM system (USM-1300s-^{3}He), STM images were acquired in the constant-current mode with a tungsten tip. Differential conductance (dI/dV) spectra were acquired by a standard lock-in amplifier at a frequency of 973.1 Hz. The tips were calibrated on a clean Nb(111) surface prepared by repeated cycles of sputtering with argon ions and annealing at 1200 ℃. Low temperature of 0.55 K is achieved by a single-shot ^{3}He cryostat. A magnetic field up to 11 Tesla can be applied perpendicularly to the sample surface.
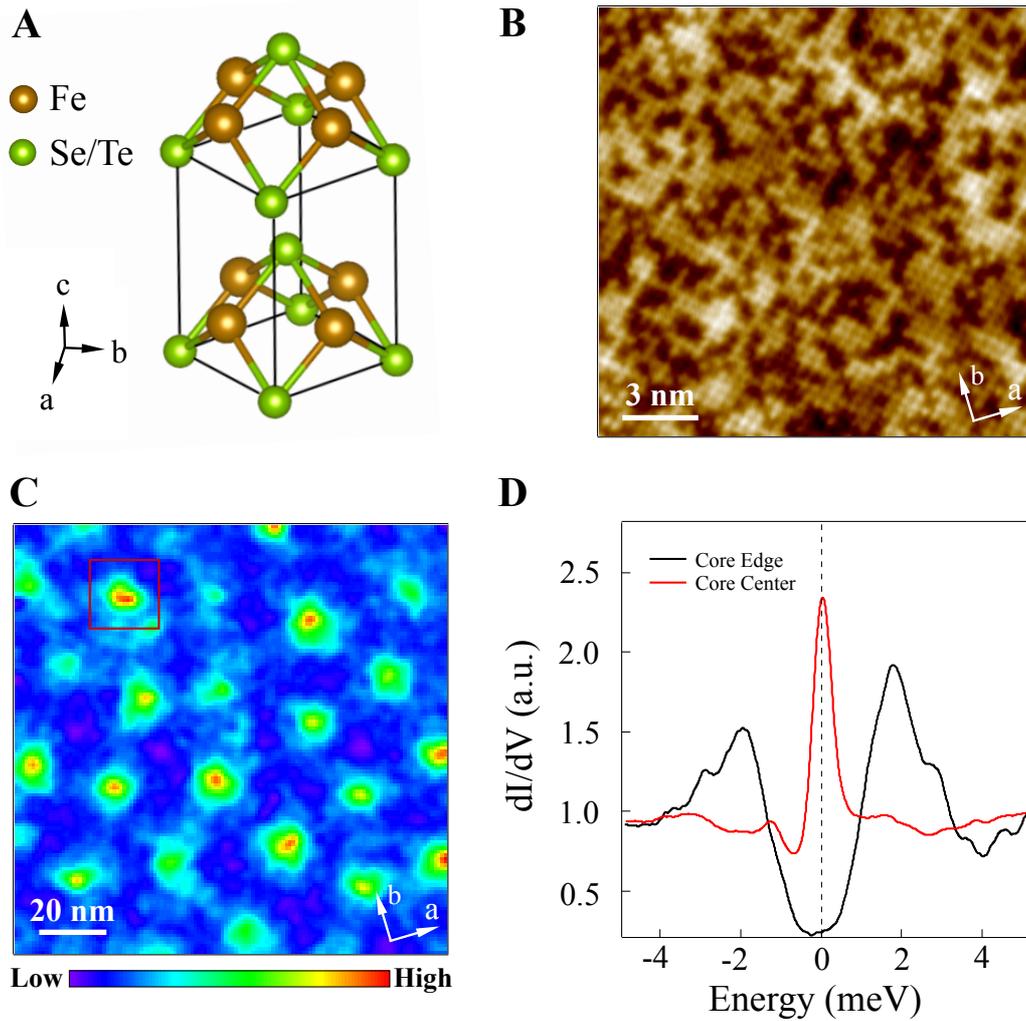
Fig.1 **Vortex cores of Fe(Te, Se).** (A) Crystal structure of Fe(Te, Se). Axis a or b indicates one of Fe-Fe bond directions. (B) STM topography of Fe(Te, Se) (sample bias: V_s = -10 mV, tunneling current: I_t = 100 pA, scanning area: 17 nm × 17 nm). (C) Normalized zero-bias conductance (ZBC) map measured at a magnetic field of 4 T, with the settings: V_s = -10 mV, I_t = 100 pA, area = 120 nm × 120 nm, showing a distorted triangular Abrikosov lattice. (D) A sharp zero-energy peak in a dI/dV spectrum measured at the vortex core center indicated in the red box on (C). It is in sharp contrast to the spectrum measured at the edge of the vortex where a two-gap feature is largely unchanged from the case of zero field.
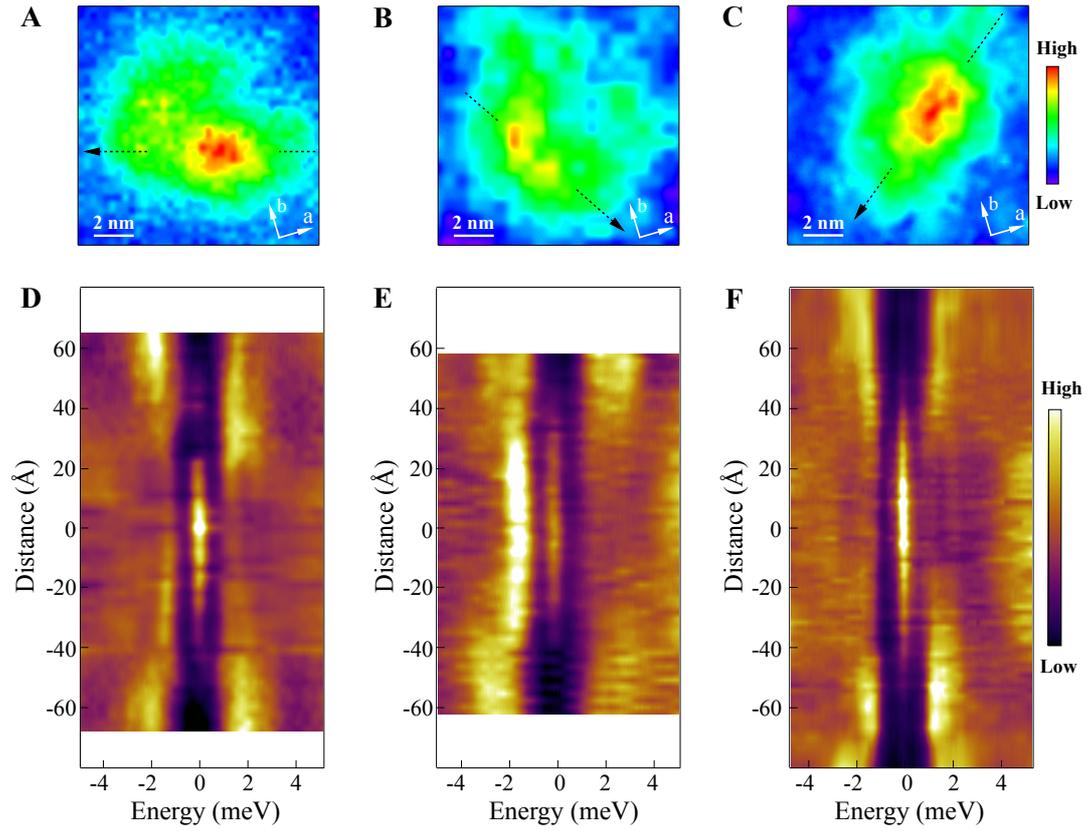
Fig.2 **Examples of zero energy peaks inside vortex core.** (A)-(C) High resolution ZBC maps (V_s = -10 mV, I_t = 100 pA, area = 12 nm × 12 nm) around three individual vortex cores. The black dash lines correspond to the line-cut intensity plots in (D)-(F), respectively. (D)-(F) Spatial profiles of these three different vortexes. The data are normalized by the integrated area of each dI/dV spectrum. The modulation bias (V_{mod}) was set to 0.2 mV, 0.2 mV and 0.08 mV, respectively.
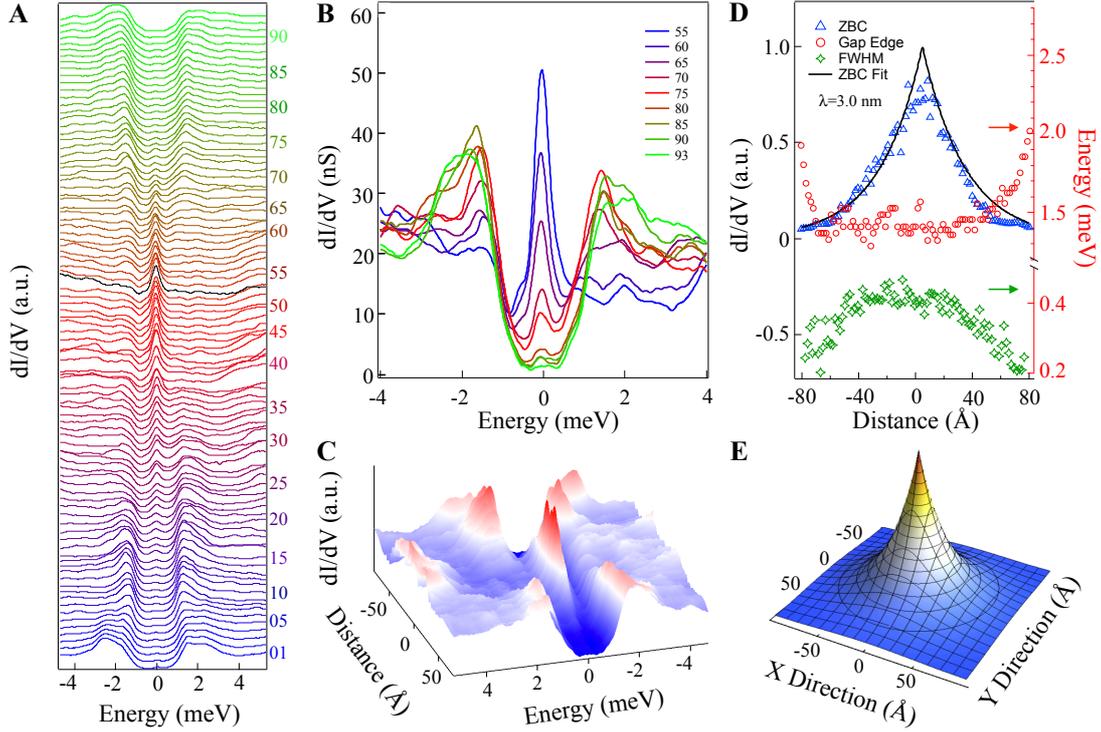
Fig.3 **Energetic and spatial profile of Majorana bound states.** (A) A waterfall-like plot of 93 spectra measured along a 160-Å line indicated at Fig. 2C. (B) A overlapping display of selected 9 dI/dV spectra. (C) Three-dimensional dI/dV(E, r) plot of Fig. 2F. (D) Spatial profile of the MBS wave function. Blue triangular symbols (line) show the experimental (fitting) spatial evolution of ZBC. The decay length derived from an exponential fitting is about 3 nm. Red circular symbols indicate the spatial evolution of gap edge. Green star symbols indicate the FWHM of MBS. (E) Reconstruction spatial distribution of Majorana bound states using the fitted decay length. This set of data is normalized by integrated area and measured with the settings: V_s = -10 mV, I_t = 100 pA, V_{mod} = 0.08 mV.
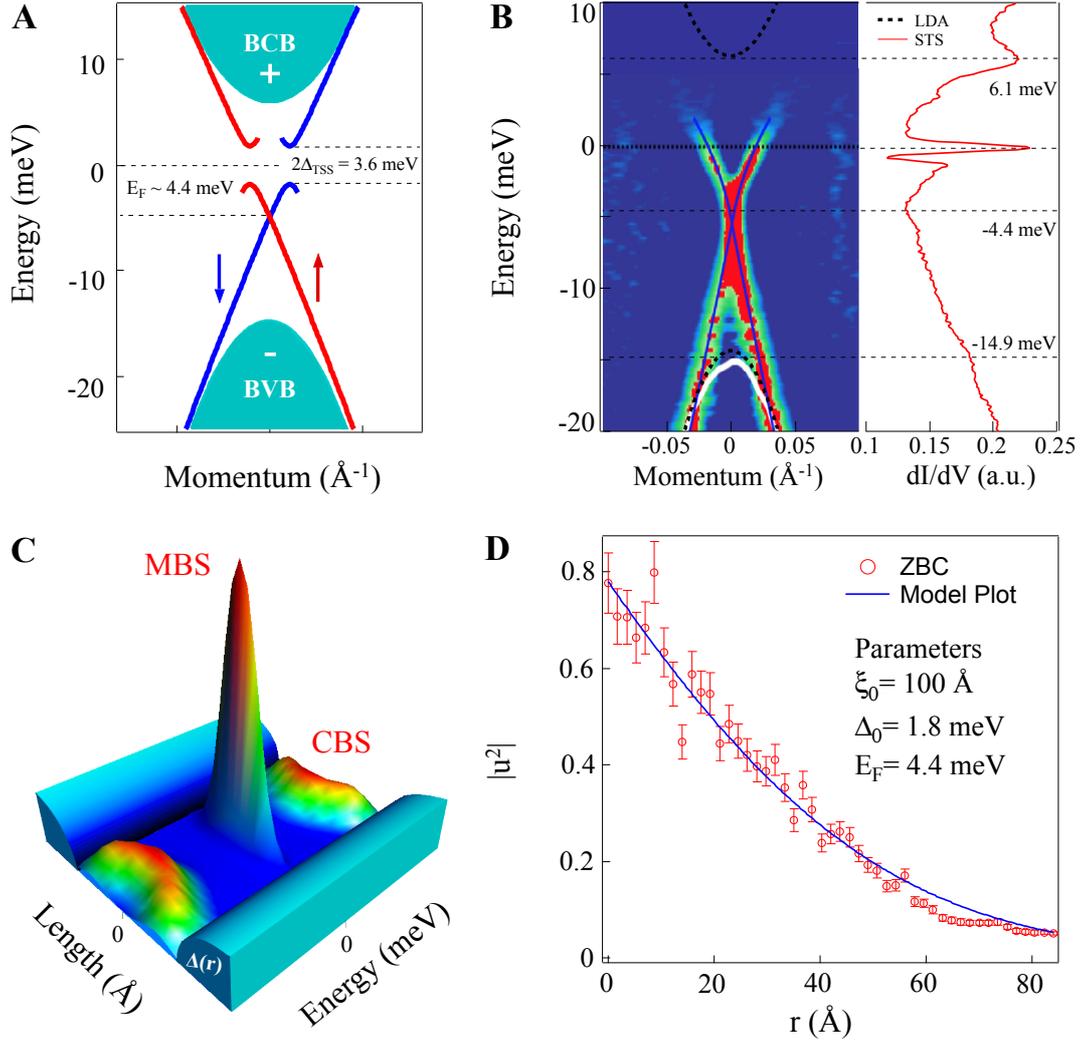
Fig.4 **Origin of pristine Majorana bound state in Fe(Te, Se).** (A) Summary of superconducting topological surface states on this material observed by ARPES from Ref. *(14)*. (B) Comparisons between ARPES and STM results. Left panel: ARPES results on the topological surface states adopted from Ref. *(14)*. Black dash curves are extracted from a LDA calculation *(23)*, with the LDA data rescaled to match the energy positions of the Dirac point and the top of bulk valance band (BVB). Right panel: a wide range dI/dV spectrum measured from -20 meV to 10 meV, showing a bump, a dip, and a peak located at -14.9 meV, -4.4 meV, 6.1 meV, respectively. (C) A schematic plot of bound states inside a vortex core. A large Δ_{sc}/E_F ratio pushes CBS away and leaves MBS residing at the zero energy largely unspoiled. (D) Comparison between the measured MBS peak intensity with a theoretical calculation of MBS spatial profile.